IEICE TRANS. FUNDAMENTALS, VOL.E86–A, NO.7 JULY 2003

LETTER *Special Section on Multi-dimensional Mobile Information Networks*

Spatial Correlation Functions for a Circular Antenna Array and Their Applications in Wireless Communication Systems

Jie ZHOU[†a)], **Shigenobu SASAKI**[†], **Shogo MURAMATSU**[†], **Hisakazu KIKUCHI**[†], ***and*** **Yoshikuni ONOZATO**[††], ***Regular Members***

SUMMARY In this paper, we derive spatial correlation functions of linear and circular antenna arrays for three types of angular energy distributions: a Gaussian angle distribution, the angular energy distribution arising from a Gaussian spatial distribution, and uniform angular distribution. The spatial correlation functions are investigated carefully. The spatial correlation is a function of antenna spacing, array geometry and the angular energy distribution. In order to emphasize the research and their applications in diversity reception, as an example, performance of the antenna arrays with MRC in correlated Nakagami fading channels is investigated, in which analytical formulas of average BER for the spatial correlation are obtained.

key words: *spatial correlated function, antenna array, Nakagami fading, MRC and diversity reception*

1. Introduction

Next generation wireless communication is based on a global system of fixed and wireless mobile services that are transportable across different network backbones [1], [2], network service providers and network geographical boundaries. In the complicated wireless environments, multi-path fading severely impairs the performance of mobile communication systems. Diversity reception [3], [4] with smart antenna arrays using signal processing method, has been recognized by most third generation wireless transmission technologies proposals as a way to enhance the capacity and the system coverage by effectively combating the multi-path fading. However, the diversity gain is reduced by the correlation of the fading signals between the antenna branches. Therefore these problems were focused in many researches such as Refs. [5] and [6].

It is well known that correlation in fading across multiple diversity results in a degradation of the diversity gain obtained. Classic work on analysis of diversity with correlated fading channels was done in Refs. [4]–[7], where they studied the special case of Rayleigh fading. Reference [7] has proposed an approach to study the effects of spatial correlation on system performance, but the approach can be only used for two correlated antenna arrays because the 2 dimensional and linear matrix transform was simply introduced for changing the correlated channels into independent channels. Reference [8] considered the uniform angle distribution and only investigated the spatial correlation. Although Gaussian spatial distribution model is proposed in Ref. [9], this paper focused on unified channel model derivations, and also investigated the spatial correlation and frequency correlation coefficients. The spatial correlation with circular antenna array geometries in Gaussian angle distribution and Gaussian spatial distribution, and the performance analysis in practical wireless channels have not been investigated.

In this paper, we derive spatial correlation functions of linear and circular antenna arrays for three types of angular energy distributions: a Gaussian angle distribution, the angular energy distribution arising from a Gaussian spatial distribution, and uniform angular distribution. The spatial correlation functions are investigated carefully. The spatial correlation is a function of antenna spacing, array geometry and the angular energy distribution. In order to emphasize the research and their applications in diversity reception, as an example, performance of the antenna arrays with Maximal Ratio Combining (MRC) in correlated Nakagami fading channels is investigated, in which analytical formulas of average Bit-Error-Rate (BER) for the spatial correlation are obtained.

The rest of this paper is organized and presented as follows. Section 2 gives the antenna array geometry and spatial vector channel model. In Sect. 3, the spatial correlation functions are derived. The numerical results are given and discussed in Sect. 4. Finally, we conclude this paper.

2. Array Geometry and Angular Energy Distribution

A. Array geometry

In antenna array system, an antenna array is used at

Manuscript received October 24, 2002.
Manuscript revised February 7, 2003.
Final manuscript received March 19, 2003.

[†]The authors are with the Department of Electrical and Electronic Engineering, Faculty of Engineering, Niigata University, Niigata-shi, 950-2181 Japan.
[††]The author is with the Department of Computer Science, Faculty of Engineering, Gunma University, Kiryu-shi, 376-8515 Japan.
a) E-mail: zhoujie45@hotmail.com

the base station to receive information from users of wireless networking operating under the same or different multiple access schemes such as FDMA, TDMA and CDMA. The antenna array may assume different geometries. In a linear array, the locations of the antennas form a straight line, whereas in a planar array (such as circular array), the positions of the antenna elements are specified by two variables representing polar or Cartesian coordinates. While the propagation delay T between antennas encountered as the signal travels across a linear array is only a function of the elevation angle, both elevation and azimuth angles of arrival define the propagation delay in the case of planar arrays. For simplicity, only azimuth plane is considered in the geometry models. Figure 1 shows the antenna array geometry used in our investigation where we have estimated a linear geometry as Fig. 1(a) and a circle of radius R as Fig. 1(b) in which the antenna elements lie about at a radius of $r = R$ for our circular antenna array.

If the antennas are widely spaced (often eight wavelength apart), then the signals received by one antenna element are likely to be independent or uncorrelated from the signals received by the adjacent antenna element of the array. This condition is due to the difference in the scattering effects on the signal amplitude

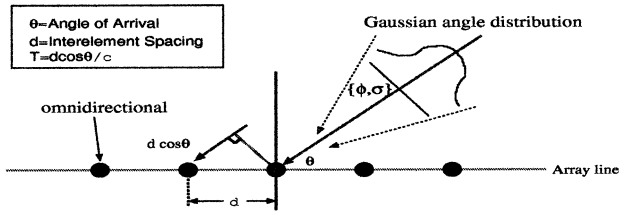

(a) Linear antenna array

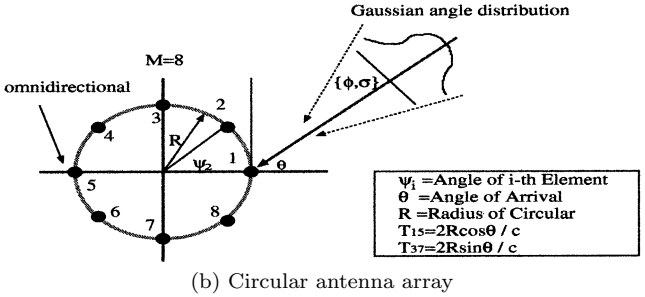

(b) Circular antenna array

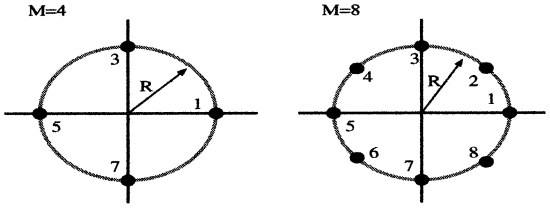

(c) 4-element antenna array and 8-element antenna array

Fig. 1 Signal angle determination in (a) linear antenna array and (b) circular antenna array, and (c) 4-element antenna array and 8-element antenna array.

and phase at different points in space, each occupied by one antenna. This space sampling method is referred to as spatial diversity. To make use of spatial diversity, the output of the antennas are compared and the antenna with the strongest signal then is chosen to feed into the receiver. However, choosing from or combining the antenna output, such as MRC investigated in this paper, when they are diverse in space is known to yield a enough improvement in the received signal.

With the antennas closely spaced (often apart by a distance smaller than or equal to half a wavelength), the waveforms incident on different antennas on longer can be assumed uncorrelated or independent. The relationship among the output level from the antennas is one of the prime characteristics of smart antennas in radio mobile communications. These outputs are linearly or nonlinearly combined through optimum or adaptive signal processing techniques to significantly increase the quality of the communication links, reduce the required amount of transmitted power and increase the number of users.

B. Angular energy distribution

The first model for a spatial channel is a Gaussian angle distribution which is commonly used [8], [9]. Thus the angular distribution function can be represented as

$$p(\theta) = \frac{\kappa}{\sqrt{2\pi}\sigma} e^{-(\theta-\phi)^2/2\sigma^2} \quad \text{for } \theta \in [-\pi+\phi, \pi+\phi] \tag{1}$$

where ϕ and σ are the mean direction of arrival and the standard deviation of the distribution. κ is the normalization factor, to make $p(\phi)$ a physical density function, i.e.

$$\kappa = \frac{1}{erf(\frac{\pi}{\sqrt{2}\sigma})} \tag{2}$$

where $erf(x) = \frac{2}{\sqrt{\pi}} \int_0^x e^{-t^2} dt$ is the error function. Note when the angular spread is small, κ is almost equal to unity.

A second model for a spatial channel which is commonly used is a Gaussian spatial distribution. This kind of distribution models the scatterers surrounding the receiver using a bi-variate Gaussian distribution in space. In other words, the scatterers have the position (x, y) with the probability as

$$p(x, y) = \frac{1}{2\pi\sigma_s} e^{-\frac{(x-x_0)^2+(y-y_0)^2}{2\sigma_s^2}} \tag{3}$$

where σ_s is the standard deviation in both x and y directions and (x_0, y_0) is the center of the distribution. To find the distribution of the angle-of-arrival, i.e. the angular energy distribution for determining the spatial distribution, we make the coordinate transform by $x = r\sin(\theta)$ and $y = r\cos(\theta)$ into Eq. (3). Further if we define $R = \sqrt{x_0^2 + y_0^2}$ and $\phi = \tan^{-1}(x_0/y_0)$, the

following formula can be obtained

$$p(\theta) = \frac{1}{2\pi} e^{-\frac{R^2}{2\sigma_s^2}} + \frac{R\cos(\theta-\phi)}{\sqrt{2\pi}\sigma_s} \cdot e^{-\frac{R^2\sin^2(\theta-\phi)}{2\sigma_s^2}} \cdot Q\left(-\frac{R\cos(\theta-\phi)}{\sigma_s}\right) \quad (4)$$

where $Q(x) = erfc(x/\sqrt{2})/2$. For simple calculation in correlated functions, Eq. (4) is nearly identical to the Gaussian angle distribution of Eq. (1) when values of $\theta - \phi$ are small. From Eq. (4), for larger R/σ_s and smaller $\theta - \phi$ we can approximate Gaussian spatial distribution using a Gaussian angle distribution as Eq. (1) in which with $\sigma = \sigma_s/R$.

Another common assumption for angular energy distribution is a uniform distribution. A uniform distribution of angular energy is defined as

$$p(\theta) = \frac{1}{2\Delta}, \text{ for } \theta \in [\phi - \Delta, \phi + \Delta] \quad (5)$$

where 2Δ is the range of angles about a central angle-of-arrival ϕ.

3. Spatial Correlated Functions and Performance Analysis

3.1 Spatial Correlated Functions

A. Linear array

As shown in Fig. 1(a), we consider a plane wave signal arriving at an linear array from angle of arrival signal θ with respect to the normal bisecting two points of interest separated by d meters. The array response vector $v(\theta)$ for linear geometry can be written as

$$v(\theta) = \begin{pmatrix} 1 \\ e^{-j2\pi\frac{d}{\lambda}\cos(\theta)} \\ e^{-j2\pi\frac{2d}{\lambda}\cos(\theta)} \\ \cdot \\ \cdot \\ \cdot \\ e^{-j2\pi\frac{(M-1)d}{\lambda}\cos(\theta)} \end{pmatrix}$$

where d and M are the antenna spacing and number of the antennas. The array spatial correlation between the m and n element of antenna array can be expressed as [1]–[3]

$$\rho(m,n) = E[v_m(\theta)v_n(\theta)^*] = \int_\theta v_m(\theta)v_n(\theta)^* p(\theta)d\theta \quad (6)$$

where $p(\theta)$ is the angular distribution function of incident signal. The real and imaginary parts of $\rho(m,n)$ for the linear arrays with uniform distribution of Eq. (5) are given [8], respectively as

$$Re[\rho(m,n)] = J_0(Z_l) + 2\sum_{k=1}^{\infty} J_{2k}(Z_l)\cos(2k\phi) \cdot \mathrm{sinc}(2k\Delta) \quad (7)$$

$$Im[\rho(m,n)] = 2\sum_{k=0}^{\infty} J_{2k+1}(Z_l)\sin((2k+1)\phi) \cdot \mathrm{sinc}((2k+1)\Delta) \quad (8)$$

In Eqs. (7) and (8), $Z_l = 2\pi\frac{(m-n)d}{\lambda}$ and $J_n(x)$ is the modified Bessel function of the first kind. If the incident signal is not the uniform distribution, the incident signal is following the Gaussian angle distribution. We can use Eq. (6) and derive in the similar way, such as the real and imaginary parts of $\rho(m,n)$ for the linear arrays with Gaussian angle distribution of Eq. (1) are described, respectively as

$$Re[\rho(m,n)] = J_0(Z_l) + 2\kappa\sum_{k=1}^{\infty} J_{2k}(Z_l)\cos(2k\phi) \cdot e^{-2k^2\sigma^2} Re[erf(\frac{\pi + i2k\sigma^2}{\sqrt{2}\sigma})] \quad (9)$$

$$Im[\rho(m,n)] = 2\kappa\sum_{k=0}^{\infty} J_{2k+1}(Z_l)\sin((2k+1)\phi) \cdot e^{-(2k+1)^2\sigma^2/2} Re[erf(\frac{\pi + i(2k+1)\sigma^2}{\sqrt{2}\sigma})] \quad (10)$$

B. Circular array

From the geometry of circular array shown in Fig. 1(b), the antenna elements are arranged to form a circular with the radius of R. Like the linear array, the array response vector $v(\theta)$ can be written as

$$v(\theta) = \begin{pmatrix} e^{-j2\pi\frac{R}{\lambda}\sin(\xi)\cos(\theta-\Psi_1)} \\ e^{-j2\pi\frac{R}{\lambda}\sin(\xi)\cos(\theta-\Psi_2)} \\ \cdot \\ \cdot \\ \cdot \\ e^{-j2\pi\frac{R}{\lambda}\sin(\xi)\cos(\theta-\Psi_M)} \end{pmatrix}$$

where R is the circular radius of antenna array shown in Fig. 1(b) and λ is the wavelength. ξ is the elevation angle where $\xi = 90$ degrees (only azimuth is considered). Ψ_i is the angle of $i-th$ element in azimuth plane. Using the same definition in Eq. (6), it is shown in the Appendix A that real and imaginary parts of the correlation function $\rho(m,n)$ with the circular geometry for the uniform distribution can be written as [8], [9]

$$Re[\rho(m,n)] = J_0(Z_C) + 2\sum_{k=1}^{\infty} J_{2k}(Z_C)\cos(2k(\phi-\gamma)) \cdot \mathrm{sinc}(2k\Delta) \quad (11)$$

$$Im[\rho(m,n)] = 2\sum_{k=0}^{\infty} J_{2k+1}(Z_C)\sin((2k+1)(\phi-\gamma)) \cdot \mathrm{sinc}((2k+1)\Delta) \quad (12)$$

where,

$$Z_C = \sqrt{Z_1^2 + Z_2^2} \tag{13}$$

In Eq. (13), $Z_1 = 2\pi\frac{R}{\lambda}[\cos(\Psi_m) - \cos(\Psi_n)]$ and $Z_2 = 2\pi\frac{R}{\lambda}[\sin(\Psi_m) - \sin(\Psi_n)]$. In Eqs. (11) and (12), $\sin(\gamma) = Z_1/Z_C$ and $\cos(\gamma) = Z_2/Z_C$. If the incident signal is not the uniform distribution, the incident signal follows the Gaussian angle distribution. As the derivation will be presented in the following Appendix B, the real and imaginary parts of $\rho(m,n)$ for the circular arrays with Gaussian angle distribution of Eq. (1) are described as

$$Re[\rho(m,n)] = \frac{\kappa}{\sqrt{\pi}} \int_{-\frac{\pi}{\sqrt{2}\sigma}}^{\frac{\pi}{\sqrt{2}\sigma}} e^{-y^2} [J_0(Z_C) + 2\sum_{k=1}^{\infty} J_{2k}(Z_C)\cos(2k(\gamma + \sqrt{2}\sigma y + \phi))]dy \tag{14}$$

$$Im[\rho(m,n)] = \frac{\kappa}{\sqrt{\pi}} \int_{-\frac{\pi}{\sqrt{2}\sigma}}^{\frac{\pi}{\sqrt{2}\sigma}} e^{-y^2} \left[2\sum_{k=0}^{\infty} J_{2k+1}(Z_C) \cdot \sin((2k+1)(\gamma + \sqrt{2}\sigma y + \phi)) \right] dy \tag{15}$$

3.2 Performance Analysis

In order to emphasize the above research in diversity reception, as an example, performance of the antenna arrays shown in Fig. 1(c) with MRC in correlated Nakagami fading channels is investigated, in which analytical formulas of average BER for the spatial correlation are obtained.

A. Physical Description

Considering a receiver with M diversity branches, let the received instantaneous signal envelope A_k at the k-th branch be characterized by the Nakagami-m distribution, with *pdf* given by [10], [11]

$$p_{A_k}(A_k) = \frac{2}{\Gamma(m_k)} \left(\frac{m_k}{\Omega_k}\right)^{m_k} A_k^{2m_k-1} e^{-\frac{m_k}{\Omega_k}A_k^2} \tag{16}$$

where $k = 1, 2, \ldots, M$. $\Gamma(.)$ is the Gamma function. $\Omega_k = mean(A_k^2)$ is the average power of k-th branch. m_k is the fading parameter. As m_k becomes smaller, the degree of fading becomes more severe. The Rayleigh distribution and one-sided Gaussian distribution are special cases with $m_k = 1$ and $m_k = 0.5$, respectively. The fading parameter m_k can be any real value greater than or equal to 0.5, but we will consider the cases of integer values of m_k only, considering that the measurement accuracy of channel is typically only of integer order.

MRC diversity combining scheme is used in our investigation. Assuming flat fading and perfect knowledge of channel, the instantaneous SNR χ at the output of MRC combiner is given by

$$\chi = \frac{E_s}{N_0}\sum_{k=1}^{M} A_k^2 = \sum_{k=1}^{M} \chi_k \tag{17}$$

where, $\chi_k = \frac{E_s}{N_0}A_k^2$ is the instantaneous input SNR per symbol for k-th branch at the MRC combiner.

In addition, for simplification we restrict our analysis to the case of identical branch fading parameters, i.e., $m_k = m$ for $k = 1, 2, \ldots, M$. Then the general expression for the characteristic function of χ is obtained from Ref. [11] in terms of the covariance matrix, Λ of correlation coefficients. That is,

$$\Phi_\chi(t) = \left| I_M - \frac{t}{m} \cdot H \cdot \Lambda \right|^{-m} \tag{18}$$

where I_M is $M \times M$ identity matrix and $H = diag\{mean(\chi_1), mean(\chi_2), \ldots, mean(\chi_M)\}$ with $mean(\chi_k)$ being the average input SNR per symbol for the k-th branch at the MRC combiner, and Λ is

$$\Lambda = \begin{pmatrix} 1 & B_{12}^* & B_{13}^* & \ldots & B_{1M}^* \\ B_{12} & 1 & B_{23}^* & \ldots & B_{2M}^* \\ \vdots & \vdots & \vdots & \vdots & \vdots \\ B_{1M} & B_{2M} & B_{3M} & \ldots & 1 \end{pmatrix}_{M\times M}$$

Here, $B_{kl} = b_{kl} + i\beta_{kl}$ and $b_{kl} = b_{lk}$, $\beta_{kl} = -\beta_{lk}$ [10], [11] which are referred as correlation coefficients and the asterisk indicates the complex conjugate. Here, the correlation coefficients are just the analytical formulas in Sect. 3.1 as $b_{kl} = Re[\rho]$ and $\beta_{kl} = Im[\rho]$.

B. BER Performance

The average BER in the presence of fading is obtained by averaging the conditional error probability over the *pdf* of χ, i.e.,

$$P_{BER} = \int_0^\infty P(e|\chi) \cdot p(\chi) \cdot d\chi \tag{19}$$

Here, as simple examples the differential binary phase-shift-keying (DBPSK) and non-coherent binary orthogonal frequency-shift-keying (NBFSK) are considered in our investigation. The conditional error probability is given by [2],

$$P(e|\chi) = \frac{1}{2}\exp(-a\chi) \tag{20}$$

where a is the parameter of modulation method. If $a = 1/2$, it corresponds to NBFSK modulation and $a = 1$, corresponds to DBPSK. Then from Eq. (19), the average BER, P_{BER} can be written as [11]

$$\begin{aligned} P_{BER} &= \frac{1}{2}\int_0^\infty \exp(-a\chi) \cdot p(\chi) \cdot d\chi \\ &= \frac{1}{2}\Phi_\chi(t)\Big|_{t=-a} \\ &= \frac{1}{2}\left| I_M + \frac{a}{m} \cdot H \cdot \Lambda \right|^{-m} \end{aligned} \tag{21}$$

4. Numerical Results

4.1 Spatial Correlated Functions

A. Linear Geometry

From Eqs. (7)–(10), we know that the spatial correlation is a function of the antenna spacing d in the linear geometry, incident angle of signal θ and the angular energy distributions. Figure 2 shows the spatial correlation for $\phi = 30$ degrees versus d/λ for a uniform angular distribution with various angular spreads Δ. It is apparent that increasing antenna separation between elements always reduces their correlation and the correlation decreased quickly as Δ increases, but with the variation in sin form. In Fig. 2, if the antenna spacing d increases, all the curves will not reach the zero point quickly for all values of $\phi \neq 0$ degrees and $\Delta \leqq 180$ degrees.

Figure 3 shows the spatial correlation for $\phi = 30$ degrees versus d/λ for a Gaussian angle distribution with various angular spreads σ. If d increases, all the curves will not reach the zero point quickly and also varies with smooth envelope vibration.

B. Circular Geometry

The correlation functions between the antenna elements in circular geometry are derived and an antenna array with 8 elements as shown in Fig. 1(b) is adopted as an example for numerical results. Please note that all the formulas can be used to evaluate the antenna arrays with many more elements. We selected the element 1 with $\Psi_1 = 0$ degrees and element 4 with $\Psi_4 = 120$ degrees as a test situation. From Eqs. (11)–(12) and (14)–(15), we know that the correlation is a function of the circular radius R, incident angle of signal θ, and the angular energy distributions. Figure 4 shows the spatial correlation for $\phi = 30$ degrees versus R for a uniform angular distribution with various Δ. It is apparent that increasing R always reduces their correlation and the correlation decreased quickly as Δ increases, but also with the variation in sin form. Figure 5 shows the spatial correlation for $\phi = 30$ degrees versus R/λ for a Gaussian angle distribution with various σ. Not like Figs. 2 and 4, all the curves are with no envelope vibration.

Summarizing the results of Figs. 2–5, it shows the correlation decreases with increasing angular spread. The largest correlation is achieved at $\Delta = 0$ and $\sigma = 0$. The consequences of this behavior of the correlation are two fold: Firstly, if the angular spread is rather small,

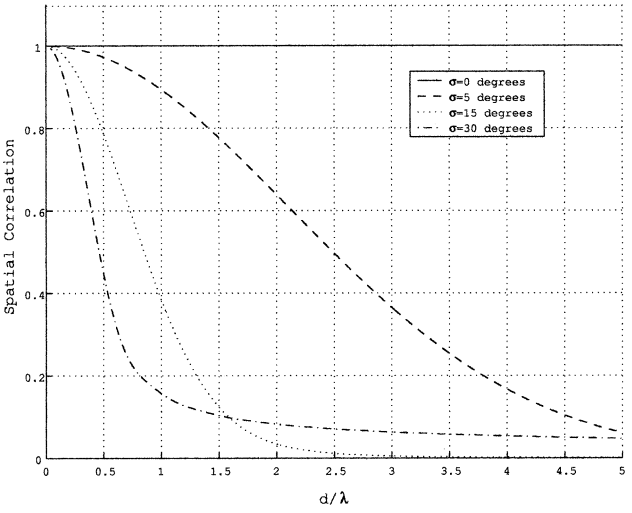

Fig. 3 Spatial correlation versus d/λ with Gaussian distribution of angular energy (ϕ=30 degrees) for linear arrays shown in Fig. 1(a).

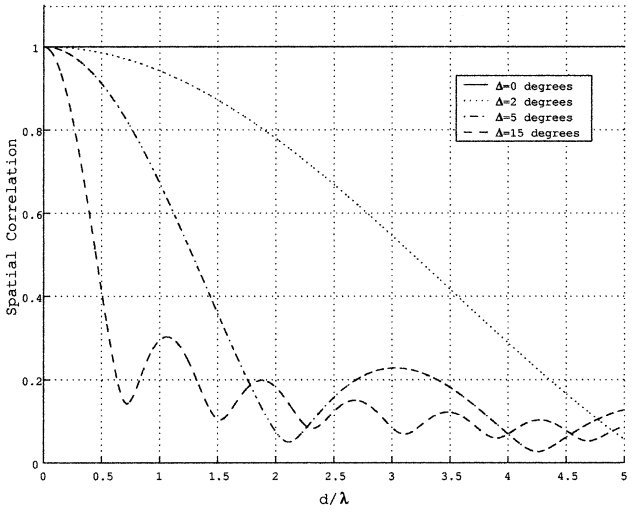

Fig. 2 Spatial correlation versus d/λ with uniform distribution of angular energy (ϕ=30 degrees) for linear arrays shown in Fig. 1(a).

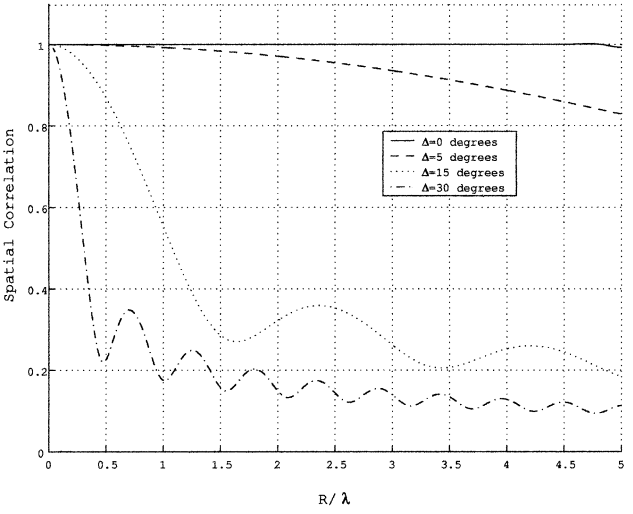

Fig. 4 Spatial correlation between the elements 1 and 4 versus R/λ with uniform distribution of angular energy (ϕ=30 degrees) for circular arrays shown in Fig. 1(b).

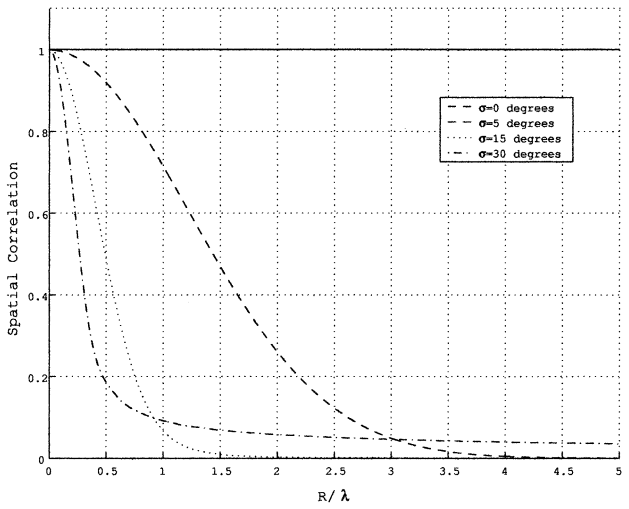

Fig. 5 Spatial correlation between the elements 1 and 4 versus R/λ with Gaussian distribution of angular energy (ϕ=30 degrees) for circular arrays shown in Fig. 1(b).

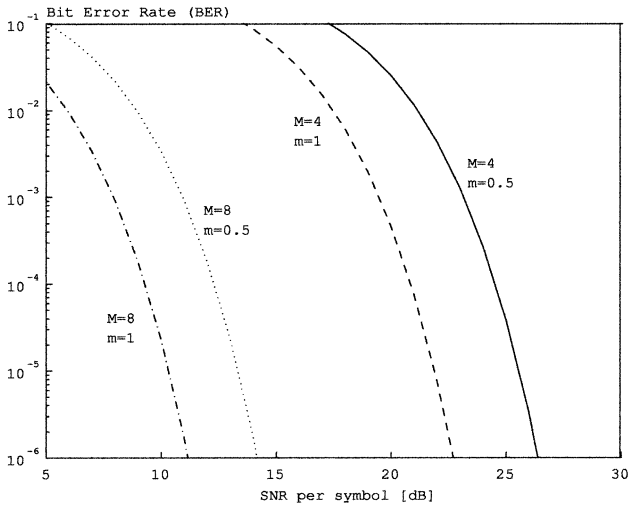

Fig. 6 BER Performance versus SNR per symbol with Gaussian angle distribution for circular antenna arrays shown in Fig. 1(c) (DBPSK a=1, $R/\lambda = 1/4$, $\sigma = 30$ degrees and $\phi = 30$ degrees).

the output signals of the elements of the antenna array are strongly correlated. In this situation, if one antenna element is in a fading dip, all others will be in the same dip too. No diversity gain can be provided in this situation. Secondly, if the angular spread is rather large, the signals of different elements of the antenna array are only weakly correlated. The signals can be combined by using various combining algorithms, such as MRC, Selection Diversity and Equal Gain Combining. The antenna array is effective as a diversity arrangement and the better diversity gain can be obtained.

Here, although the numerical results for a Gaussian spatial distribution defined as Eq. (3) are not given, the formulas for using a Gaussian angle distribution to model the Gaussian spatial distribution have been derived. Therefore we can make the relative translation to approximate a Gaussian spatial distribution with an equivalent Gaussian angle distribution by the equivalent Eq. (4).

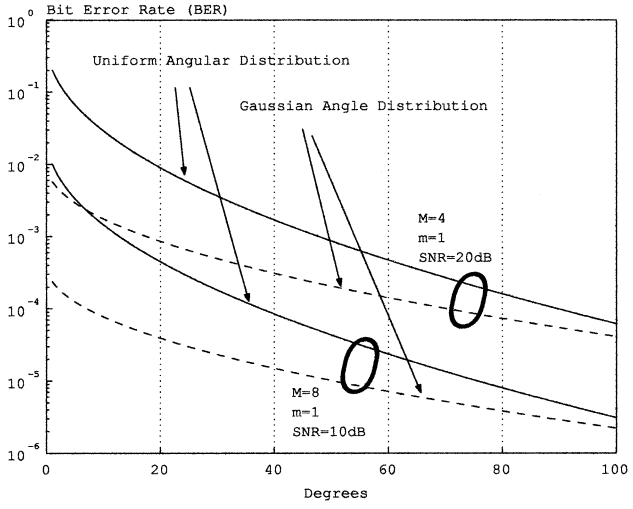

Fig. 7 BER Performance versus σ and Δ for circular antenna arrays shown in Fig. 1(c) (DBPSK a=1, $R/\lambda = 1/4$ and $\phi = 30$ degrees).

4.2 Results of BER for Circular Antenna Arrays

A. BER performance with Gaussian angle distribution

Figure 6 shows the average BER of DBPSK for $M = 4, 8$ branches, circular geometry shown in Fig. 1(c), MRC combining, with $R = 1/4\lambda$, a Gaussian angle distribution with fixed angular spread $\sigma = 30$ degrees, in $m = 0.5$ (Gaussian channel) and $m = 1$ (Rayleigh channel) fading channels. The diversity gain can be obtained by increasing from $M = 4$ to $M = 8$. We can see when $M = 8$ and $m = 1$ in Rayleigh fading channel, BER performance will be greatly improved compared with $M = 4$. For comparison, from Ref. [11] the required SNR is 35 dB as $BER = 10^{-3}$ and $m = 1$ at the case for no diversity ($M = 1$). The diversity gain is near 16.5 dB for $M = 4$ and 28.5 dB for $M = 8$ when the antenna elements are arranged in a circular antenna array shown in Fig. 6.

B. Sensitivity to σ and Δ

Figure 7 shows the average BER of DBPSK for $M = 4, 8$ versus the angular spread σ and Δ respectively, at fixed SNR in $m = 1$ fading channels. Since large angular spread σ and Δ reduce the correlation, the average BER decreases. With the increasing of the angular spread, BER difference for the uniform angular distribution and Gaussian angle distribution will be smaller and converge on the same values according to the numerical results. It should be noted that the antenna array with Gaussian angle distribution can give better

performance at $\sigma = \Delta$. BER performance can be improved by increasing M. However the use of a large M is often restricted by the implementation complexity. This means the BER performance improvement for a small M is the most significant.

5. Conclusions

In this paper, we have derived generalized spatial correlation functions for three distributions of angular energy for a linear antenna array and a circular antenna array. The generalized formulas allow the correlation to be found for any practical standard deviation and antenna array geometry. To emphasize the work, we also investigate the average BER performance of a circular antenna array with MRC combining in Nakagami fading environment. The numerical results clearly illustrate the flexibility of this analysis in determining the effects of compact antenna array configuration and the operational wireless environment. These results also will be used and play the key role in designing smart antenna systems use signal processing methods in conjunction with multiple antennas to achieve significant improvements in capacity and range for wireless mobile communications.

References

[1] W.C. Jakes, ed., Microwave mobile communications, Wiley, New York, 1974.
[2] J.G. Proakis, Digital communications, McGraw-Hill Higher Education, Thomas Casson, 2000.
[3] J.H. Winters, "The diversity gain of tarnsmit diversity in wireless systems with reyleigh fading," Proc. IEEE International Conference on Communications (ICC'95), vol.2, pp.1121–1125, May 1995.
[4] S.M. Alamouti, "A simple transmit diversity technique for wireless communications," IEEE J. Sel. Areas Commun., vol.16, no.8, pp.1451–1458, Oct. 1998.
[5] A.F. Naguib, Adaptive antenna for CDMA wireless network, PhD Thesis, Standford University, Palo Alto, CA, Aug. 1996.
[6] T. Fulghun and K. Molnar, "The jakes fading model incorporating angular spread for a disk of scatters," Proc. IEEE Veh. Technol. Conference (VTC'98), pp.489–493, May 1998.
[7] L. Fang, G. Bi, and A.C. Kot, "New method of performance analysis for diversity reception with correlated rayleigh-fading signals," IEEE Trans. Veh. Technol., vol.49, no.5, pp.1807–1812, Sept. 2000.
[8] J.A. Tsai and B.D. Woerner, "The fading correlation function of a circular antenna array in mobile radio environment," Proc. IEEE Global Telecommunications Conference (Globecom'01), San Antonio, Texas, USA, Nov. 2001.
[9] J. Fuhl, A.F. Molisch, and M. Bonek, "Unified channel model for mobile radio systems with smart antennas," IEE Proc.-Radar, Sonar Navig., vol.145, no.1, pp.32–41, Feb. 1998.
[10] J. Luo and J.R. Zeidler, "A statistical simulation model for correlated nakagami fading channels," Proc. International Conference on Communications Technology (ICCT'2000), vol.2, pp.1680–1684, Beijing, China, Aug. 2000.
[11] J. Luo, J.R. Zeidler, and S.M. Laughlin, "Performance analysis of compact antenna arrays with maximal ratio combining in correlated nakagami fading channels," IEEE Trans. Veh. Technol., vol.50, no.1, pp.267–277, Jan. 2001.

Appendix A: Derivation of Spatial Correlation Function for Uniform Distribution

As description in Sect. 2-B, we wish to show that spatial correlation function for a circular antenna array when the arrival signals are following a uniform angular energy distribution. According to the definition of correlation function in Eq. (6) and the uniform distribution function shown in Eq. (5), we can obtain the correlation function formula as

$$\begin{aligned}\rho(m,n) &= \int_{\theta} v_m(\theta) v_n(\theta)^* p(\theta) d\theta \\ &= \frac{1}{2\Delta} \int_{\phi-\Delta}^{\phi+\Delta} e^{-j2\pi \frac{R}{\lambda}(\cos(\theta-\Psi_m)-\cos(\theta-\Psi_n))} d\theta \end{aligned} \tag{A·1}$$

If we define $Z_1 = 2\pi\frac{R}{\lambda}[\cos(\Psi_m) - \cos(\Psi_n)]$ and $Z_2 = 2\pi\frac{R}{\lambda}[\sin(\Psi_m) - \sin(\Psi_n)]$. So $Z_C = \sqrt{Z_1^2 + Z_2^2}$ can be defined. Let $\sin(\gamma) = Z_1/Z_C$ and $\cos(\gamma) = Z_2/Z_C$, then Eq. (A·1) can be transformed as

$$\rho(m,n) = \frac{1}{2\Delta} \int_{\phi-\Delta+\gamma}^{\phi+\Delta+\gamma} e^{-jZ_C \sin(\zeta)} d\zeta \tag{A·2}$$

where $\zeta = \gamma + \theta$. In this formula, $e^{-jZ_C \sin(\zeta)} = \cos(Z_C \sin(\zeta)) - j\sin(Z_C \sin(\zeta))$ can be expressed by the modified Bessel functions as follows

$$\begin{aligned}\cos(Z_C \sin(\zeta)) &= J_0(Z_C) + 2\sum_{k=1}^{\infty} J_{2k}(Z_C)\cos(2k\zeta) \\ \sin(Z_C \sin(\zeta)) &= 2\sum_{k=0}^{\infty} J_{2k+1}(Z_C)\sin((2k+1)\zeta)\end{aligned} \tag{A·3}$$

After substituting Eq. (A·3) into Eq. (A·2) and integrating it, the real and imaginary parts of the correlation function $\rho(m,n)$ of circular antenna arrays for a uniform distribution can be expressed as Eqs. (11) and (12).

Appendix B: Derivation of Spatial Correlation Function for Gaussian Angle Distribution

As the same derivation in Appendix A, we derive correlation function of the circular antenna array for a Gaussian angle distribution, Eqs. (14) and (15) in this Appendix. First, let us assume a Gaussian distribution for angular energy such that the distribution function can

be represented as Eq. (1) as follows

$$p(\theta) = \frac{\kappa}{\sqrt{2\pi}\sigma} e^{-(\theta-\phi)^2/2\sigma^2} \quad \text{where, } \theta \in [-\pi+\phi, \pi+\phi] \tag{A·4}$$

where κ is the normalization factor that is expressed by Eq. (2), to make $p(\theta)$ a physical density function.

Then like the same definitions in Appendix A, we know that the spatial correlation function can be determined as

$$\rho(m,n) = \frac{\kappa}{\sqrt{2\pi}\sigma} \int_{-\pi+\phi}^{\pi+\phi} e^{-(\frac{\theta-\phi}{\sqrt{2}\sigma})^2} e^{-jZ_C \sin(\gamma+\theta)} d\theta \tag{A·5}$$

If we let $\chi = \frac{\theta-\phi}{\sqrt{2}\sigma}$, then the parameter θ can be transformed as $\theta = \sqrt{2}\sigma\chi + \phi$ and make a change of variables, so $\chi \in [-\frac{\pi}{\sqrt{2}\sigma}, \frac{\pi}{\sqrt{2}\sigma}]$. Therefore we obtain

$$\begin{aligned}\rho(m,n) &= \frac{\kappa}{\sqrt{\pi}} \int_{-\frac{\pi}{\sqrt{2}\sigma}}^{\frac{\pi}{\sqrt{2}\sigma}} e^{-\chi^2} e^{-jZ_C \sin(\gamma+\theta+\sqrt{2}\sigma\chi)} d\chi \\ &= \frac{\kappa}{\sqrt{\pi}} \int_{-\frac{\pi}{\sqrt{2}\sigma}}^{\frac{\pi}{\sqrt{2}\sigma}} e^{-\chi^2} \cos(Z_C \sin(\gamma+\theta+\sqrt{2}\sigma\chi)) d\chi \\ &+ \frac{\kappa}{\sqrt{\pi}} \int_{-\frac{\pi}{\sqrt{2}\sigma}}^{\frac{\pi}{\sqrt{2}\sigma}} e^{-\chi^2} \cos(Z_C \sin(\gamma+\theta+\sqrt{2}\sigma\chi)) d\chi\end{aligned} \tag{A·6}$$

Now, substituting Eq. (A·4) into Eq. (A·6), we can get the real and imaginary parts of $\rho(m,n)$ equations shown as Eqs. (14) and (15).